АТОМНА ЕНЕРГЕТИКА
ATOMIC ENERGY

УДК 621.039 https://doi.org/10.15407/jnpae2021.03.243

O. G. Diakov, I. A. Maliuk, D. P. Stratilat, M. V. Strilchuk*, V. V. Tryshyn

Institute for Nuclear Research, National Academy of Sciences of Ukraine, Kyiv, Ukraine

*Corresponding author: myst@kinr.kiev.ua

CALCULATION OF SPECTRUM AND NEUTRON FLUX DENSITY IN EXPERIMENTAL CHANNELS OF WWR-M REACTOR

A program for calculating the spectra and densities of neutron fluxes in the experimental channels of the research reactor WWR-M was developed. To do this, the reactor core was modeled. Irradiation of neutron activation detectors was performed. The obtained experimental rates of nuclear reactions are consistent with the calculated within 10 %.

Keywords: research reactor, Geant4, neutron spectrum, neutron flux density, neutron activation detector, reaction rate.

1. Introduction

Nuclear research reactors are used as a powerful source of neutrons for both fundamental and applied studies, including silicon doping, neutron activation analysis, radiopharmaceuticals production, irradiation of structural materials, and nuclear fuel testing. It requires the correct knowledge of both neutron spectrum and neutron flux density in the point of irradiation. These characteristics can be changed and strongly depend on the configuration of the reactor core formed for a particular task.

This paper proposes an experimental-computational approach to determine the characteristics of neutron fields at any point for a given configuration of the reactor core. The approach involves the reactor core modeling and the calculation of neutron flux density and neutron spectrum at a given point by the Monte Carlo method taking into account the specific design of the nuclear reactor, and then by comparing the calculation results with the data obtained by neutron activation detectors. To be successfully used, the approach requires measuring the nuclear reaction rates in the neutron detectors with uncertainties less than 3 %, applying the optimal set of the neutron detectors to characterize the entire energy range of the neutron fields, and finally knowing the most accurate values of all used nuclear reaction cross sections.

2. Modeling of the WWR-M reactor

Phantom model is designed using the GEANT4-10-5 libraries [1]. The libraries have a set of algorithms and data, including cross-sections of nuclear-physical processes, and allow you to simulate the processes induced by particles passing through an experimental setup, to track various parameters of the particle trajectory, and to obtain the detector response as well. Particle trajectories and experimental setup can be presented graphically. Thus, the GEANT4 allows you to describe the geometry of the real setup and its component materials, moreover it can be easily adapted to accomplish this task. Other codes, such as the MCNP, which are better suited for their intended purposes, have a limited set of simulation output data, and it is difficult to apply these codes for tasks outside of their scope.

The modeling of nuclear interactions used the physical model QGSP_BERT_HP, which includes the model of intranuclear cascades Bertini, the model of pre-equilibrium decays, the evaporation model, and models of high-precision neutron processes with energies below 20 MeV as well. The ThermalNeutronScattering model was used to describe the elastic scattering of thermal neutrons with energies below 4 eV.

Nuclear data include cross-sections of interaction, initial angular and energy distributions, and the formation of secondary particles. Because experimental nuclear data are incomplete, the estimated datasets are formed using a combination of experimental data, nuclear interaction models, and expert evaluations. The ENDF/B-VIII.0 (2018) database was used in this work.

The reactor model, created by the software and shown in Fig. 1, includes:

beryllium reflector;

fuel assemblies, the design of which corresponds to their technical specifications, with the burnup averaged over all assemblies for the period 2011 - 2019. To obtain the spatial distributions of the released energy and neutron fluxes, all elements of the reactor core are divided into 20 layers in height. The area of the fuel assembly containing uranium consists of 16 layers in height;

beryllium displacers;

emergency protection rods with boron carbide neutron absorber;

control rods, the position of which is set for required reactor power;

an experimental channel, where 16 neutron activation detectors are placed.

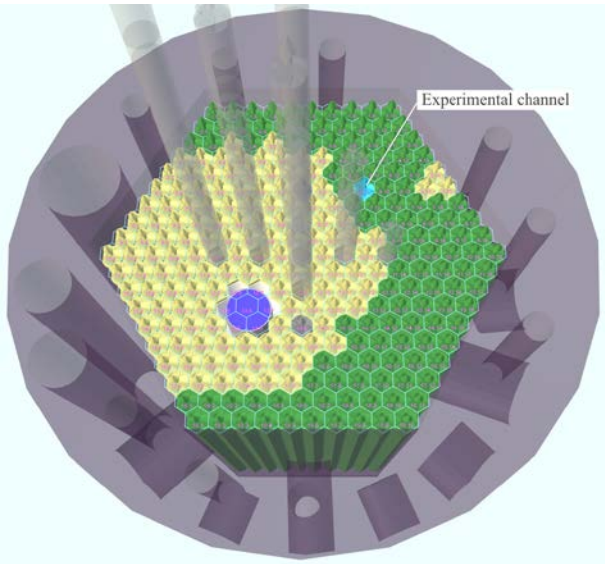

Fig. 1. WWR-M reactor model. ▢ - fuel assemblies, ▢ - beryllium displacers, ▢ - beryllium reflector, ▢ - emergency and control rods.
(See color Figure on the journal website.)

Since the Monte Carlo simulation considers the motion of individual particles, the simulation should begin with a set of initial neutrons. In our model, the initial neutrons were emitted by fuel assemblies and thus correspondingly they had a fission spectrum of ^{235}U. The probability of neutron emition was the same for each elementary volume of the assembly, moreover isotropic and stable. The Monte Carlo simulation is a stochastic process, so the statistical accuracy of the results will be proportional to the number of initial neutrons. The most simulation results are discrete, therefore they obey Poisson's law, and the uncertainty would be $\sqrt{N}$, where N is the number of registered events.

To assess the criticality of the reactor K_{eff}, defined as the ratio of the number of neutrons of one generation to the number of neutrons of the previous generation, a static calculation method was used. This approach provides quite accurate criticality assessment when the simulation of a system such as the nuclear reactor operated at steady power level is performed. For non-critical systems, the approach can be used to qualitatively assess whether a system is supercritical or subcritical. For the given configuration of the reactor core and position of the control rods, the value of K_{eff} is equal to 0.999, thus it is close to 1 and additionally confirms the correctness of the reactor core model.

When neutrons hit an elementary volume, the program counts their number. As a result, we obtain the neutron fluence averaged over the elementary volume. If the obtained fluence (expressed in cm^{-2}) is normalized to the ratio of the actual thermal power of the reactor, obtained from the operational log, to the energy, deposited in all elementary volumes of the model as a result of fission events, we obtain the neutron flux density expressed in the units of $cm^{-2}\cdot s^{-1}$. Fig. 2 shows the distribution of neutron flux density in the reactor core at a power of 1,116 MW.

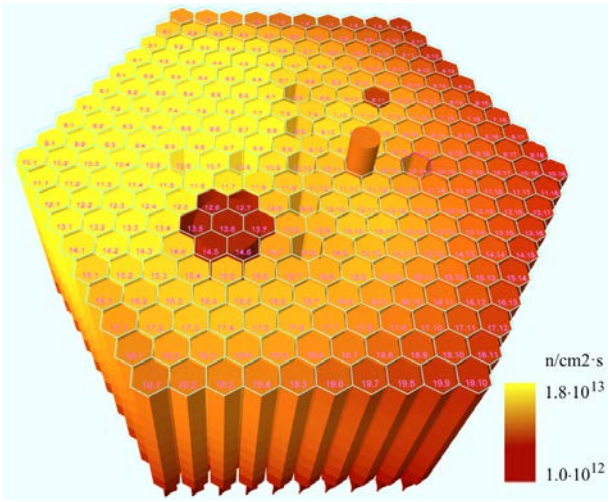

Fig. 2. Neutron flux density distribution.
(See color Figure on the journal website.)

Models of activation detectors placed in the experimental channel were enhanced to increase the statistical accuracy, which is especially important for the formation of neutron spectra, and the actual size was 3×3 cm^2. The average values of neutron flux density in the activation detectors are shown in Table 1 (the positions of the activation detectors are given relative to the center of the reactor core).

Table 1. **Distribution of neutron flux densities in the activation detectors**

The relative vertical position of the detector, mm	Flux density, n/(cm^2·s)	The relative vertical position of the detector, mm	Flux density, n/(cm^2·s)
–234.375	$8.606\cdot10^{12}$	15.625	$1.554\cdot10^{13}$
–203.125	$1.043\cdot10^{13}$	46.875	$1.521\cdot10^{13}$
–171.875	$1.196\cdot10^{13}$	78.125	$1.464\cdot10^{13}$
–140.625	$1.326\cdot10^{13}$	109.375	$1.378\cdot10^{13}$
–109.375	$1.428\cdot10^{13}$	140.625	$1.265\cdot10^{13}$
–78.125	$1.500\cdot10^{13}$	171.875	$1.127\cdot10^{13}$
–46.875	$1.544\cdot10^{13}$	203.125	$9.724\cdot10^{12}$
–15.625	$1.562\cdot10^{13}$	234.375	$8.075\cdot10^{12}$

16 neutron spectra were acquired by the activation detectors. The spectra in the points of maximum and minimum neutron flux density are presented in Fig. 3.

The configuration parameters of all reactor elements are stored in the database. The results of modeling – the energy release and the neutron flux densities in elementary volumes of the reactor core are also entered into the database. Typically, the neutron spectra are formed for the activation detectors, but it is possible to obtain the spectrum record for any object in the reactor core.

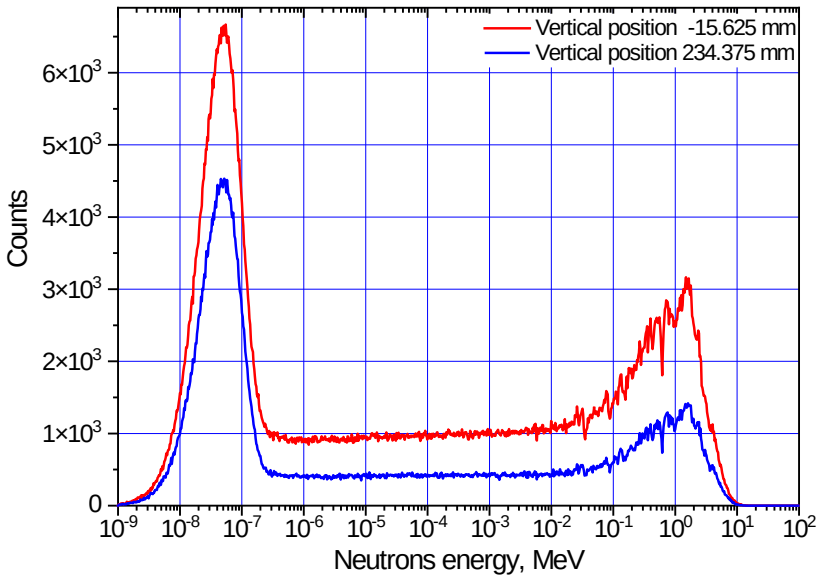

Fig. 3. Neutron spectra.
(See color Figure on the journal website.)

To visualize both DirectX modeling of the reactor core and the obtained results, the three-dimensional model, which maximally corresponds to the model used in the Geant4 calculations, was developed.

After ~ 10^8 simulations, we obtained as the radial distribution of the released energy in the reactor core (Fig. 4), as the vertical energy distribution (Fig. 5).

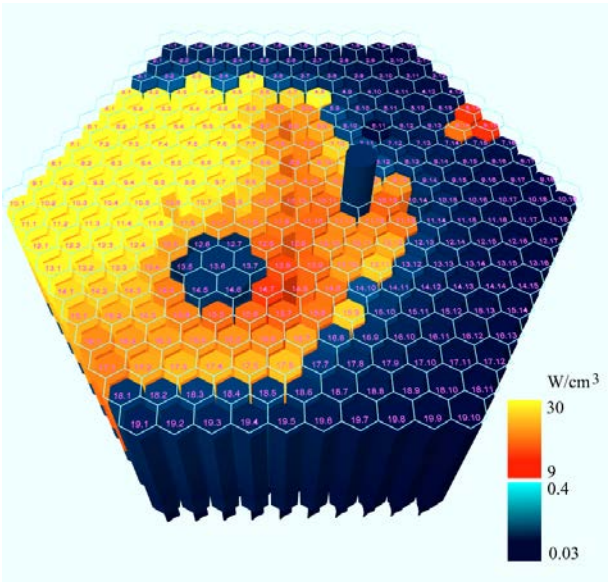

Fig. 4. Radial energy distribution.
(See color Figure on the journal website.)

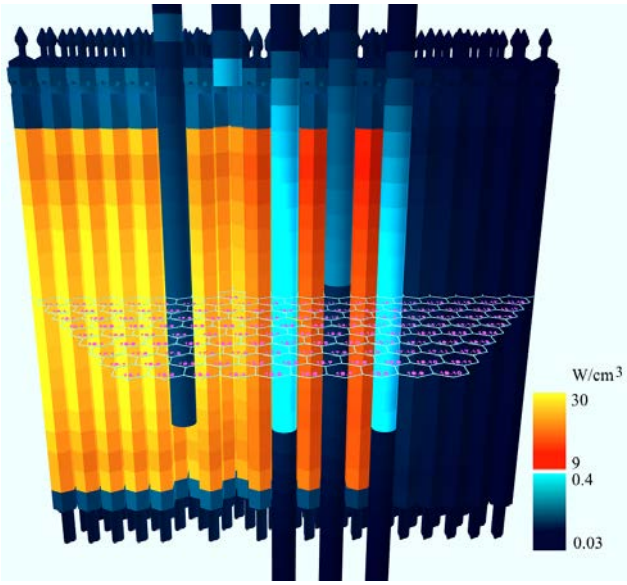

Fig. 5. Vertical energy distribution.
(See color Figure on the journal website.)

3. PhantomGun code

Even though the simulation of the reactor was performed by us on a modern computer using multithreading, only activation detectors with large nuclear reaction cross sections can be directly irradiated in the reactor model. Therefore, we developed both code and the model in which the activation detectors with an area of 1 cm^2 and a thickness corresponding to the actual thickness of the detectors were irradiated by neutrons, while the isotropic angular distribution of primary particles was used to reproduce the real radiation distribution in the reactor core, as shown in Fig. 6. To verify the correctness of the model, we irradiated a sample of Mn directly in the reactor model and the PhantomGun code. Within statistical uncertainty, we obtained the same results.

The neutron flux density and the neutron spectrum for each activation detector were calculated by the PhantomGun code and selected from the database. To control the correct operation of the neutron generator the code accumulated a spectrum of neutrons passing through the activation detector as well.

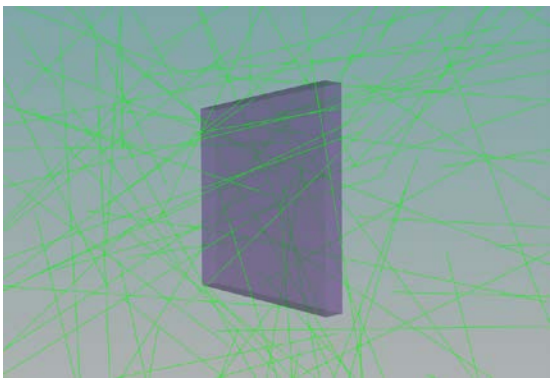

Fig. 6. Modeling of the irradiation of activation detectors by the PhantomGun code. (See color Figure on the journal website.)

As a result of the simulation, we obtained all nuclear reaction rates for the activation detector R. As an example, Table 2 shows the results for the irradiation of nickel foil with a thickness of 50 μm in a vertical position −15.625 mm from the center of the reactor core.

Table 2. **The results for the irradiation of nickel foil obtained by the PhantomGun code**

Nuclei	The nuclear reaction rate R, 1/s per 1 nucleus of the element
^{57}Fe	$6.406 \cdot 10^{-16}$
^{58}Co	$2.964 \cdot 10^{-13}$
^{60}Co	$2.135 \cdot 10^{-15}$
^{65}Ni	$1.775 \cdot 10^{-13}$

4. Measurement of neutron reaction rates with the activation detector

To verify the correctness of the calculations for neutron fluxes and spectra performed by the Phantom code, the activation detectors of Mn, Au, Lu, and Ni were irradiated in the activation channels of the nuclear reactor operated at the power of 1,116 MW.

After the irradiation, γ-ray spectra of the activation detectors were measured and the corresponding nuclear reaction rates per 1 nucleus of the element, R were calculated as follows:

$$R = \frac{A_{mes}}{N_n} \frac{1}{\left(1 - e^{-\lambda t_{irr}}\right) \cdot e^{-\lambda t_{exp}}}, \qquad (1)$$

where: R - nuclear reaction rate (s^{-1}/nuclei); A_{mes} - activity of the sample at the beginning of the measurements (Bq); N_n - number of nuclei of the target element in the sample; λ - decay constant of the reaction product, s^{-1}; t_{irr} - irradiation time of the sample, s; t_{exp} - exposure time of the sample before the start of measurements, s.

While the A_{mes} is calculated by the formula:

$$A_{mes} = \frac{S\lambda}{\varepsilon_\gamma I_\gamma \left(1 - e^{-\lambda t_{mes}}\right)}, \qquad (2)$$

where: S - area of the total absorption peak for the analyzed gamma transition; ε_γ - absolute registration efficiency for the analyzed gamma transition; I_γ - quantum yield for the analyzed gamma transition; t_{mes} – "live" sample measurement time, s.

5. Comparison of the calculated and experimental data

The nuclear reaction ^{55}Mn(n, γ)^{56}Mn (Fig. 7) was chosen for such comparison because it has no resonances with large cross-sections and its rates are totally determined by the thermal neutrons.

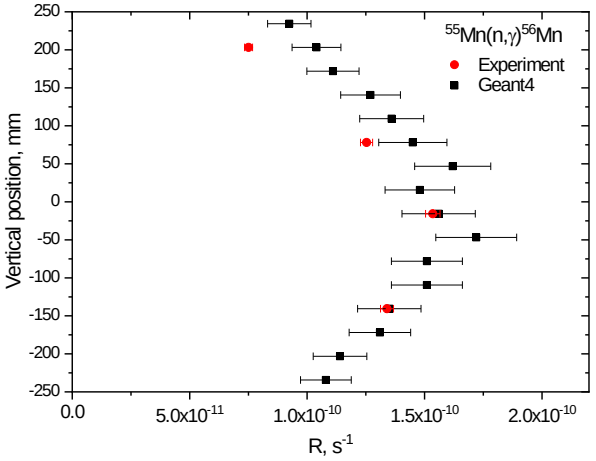

Fig. 7. The calculated and experimental rates for ^{55}Mn(n, γ)^{56}Mn reaction. Uncertainties are given for k = 1.

At the same time, the reaction ^{176}Lu(n, γ)^{177}Lu (Fig. 8) was chosen due to the presence of strong resonance on the right slope of the thermal neutron peak. Thus, the nuclear reaction rate depends on the temperature of the neutron gas.

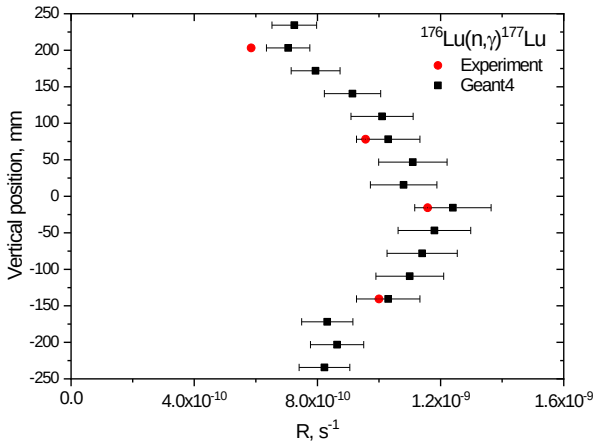

Fig. 8. The calculated and experimental rates of ^{176}Lu(n, γ)^{177}Lu reaction.

In the reaction ^{197}Au(n, γ)^{198}Au, a strong resonance with the energy of ~ 5 eV is observed, which corresponds to the beginning of the energy region of epithermal neutrons. The yield of such reaction depends on the ratio of the fluxes of thermal and epithermal neutrons. A comparison of the calculated and experimental rates of ^{197}Au(n, γ)^{198}Au reaction is shown in Fig. 9.

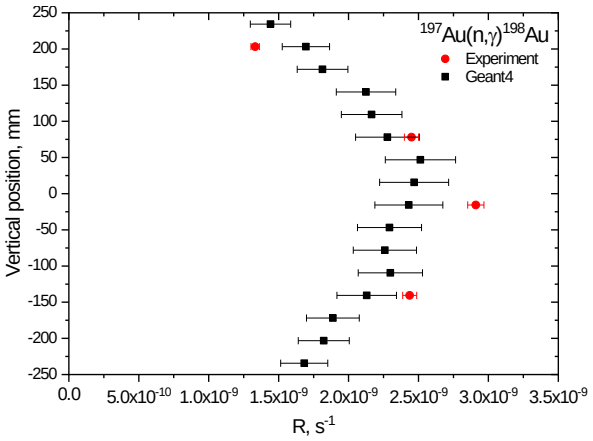

Fig. 9. The calculated and experimental rates of ^{197}Au(n, γ)^{198}Au reaction.

The reaction ^{64}Ni(n, γ)^{65}Ni has a number of resonances with large cross-sections in the high-energy part of the epithermal region, so in order to calculate correctly the reaction rate during the modeling, the energy spectrum of neutrons must be reproduced as precisely as possible (Fig. 10).

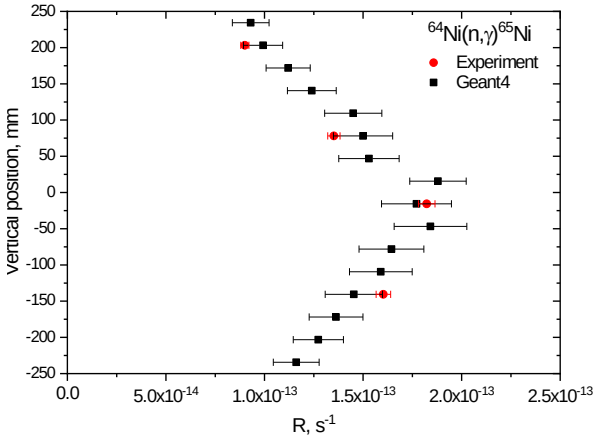

Fig. 10. The calculated and experimental rates of ^{64}Ni(n, γ)^{65}Ni reaction.

The reaction ^{58}Ni(n, p)^{58,58m}Co was used to compare the experimental and calculated values of the nuclear reaction rates for the fast neutrons. It is impossible to separate experimentally the decays of the isomer and the ground state of ^{58}Co due to the low quantum yield of the isomeric transition. Therefore, for the reaction modeling we used the total cross-section of two reactions – ^{58}Ni(n, p)^{58}Co and ^{58}Ni(n, p)^{58m}Co [2] (Fig. 11).

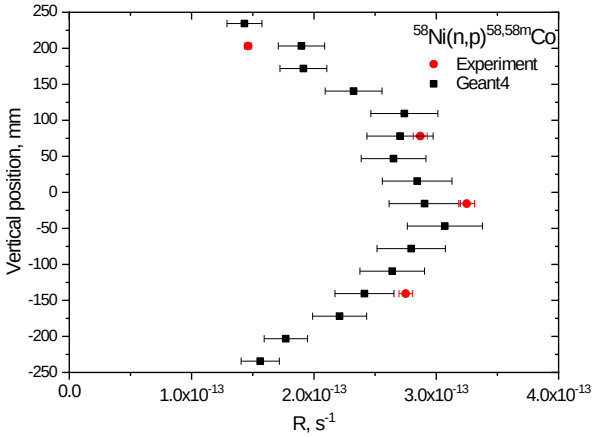

Fig. 11. The calculated and experimental rates of ^{58}Ni(n, p)^{58,58m}Co reaction.

6. Neutron flux densities in the experimental channel

To obtain the flux densities of thermal, epithermal, and fast neutrons, the neutron flux densities for each vertical position were distributed between the mentioned 3 groups of neutrons proportionally to the ratio of the counts in the corresponding energy range and the counts in the total spectrum. The distribution of flux density for the neutrons with different energies versus the vertical position is presented in Fig. 12.

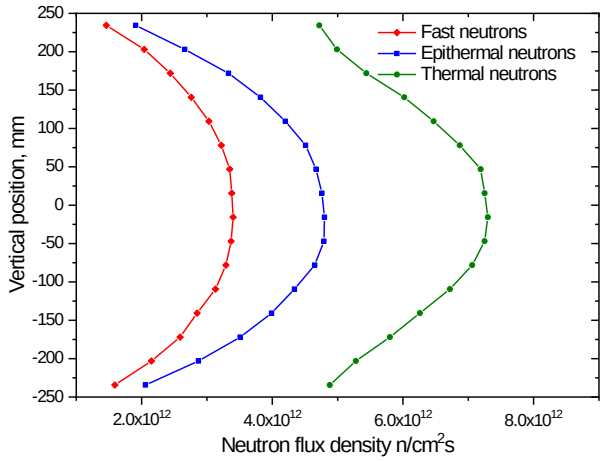

Fig. 12. Neutron flux densities.
Thermal neutrons – $1\cdot10^{-9}$ - $5\cdot10^{-7}$ MeV,
epithermal neutrons – $5\cdot10^{-7}$ - $1\cdot10^{-1}$ MeV,
fast neutrons – $1\cdot10^{-1}$ - $1\cdot10^{1}$ MeV.
(See color Figure on the journal website.)

7. Conclusions

1. A model of the WWR-M reactor was developed using the Geant4 libraries.

2. The neutron spectra and flux densities in the experimental channel were calculated.

3. The irradiation and measurement of the neutron activation detectors for 4 positions over the height of the reactor core were performed.

4. The comparison of experimental and simulated values of the reaction rates in neutron activation detectors is carried out. For the lower and middle regions of the reactor core, the experimental and calculated data agree within the uncertainty of around 10 % and it is mainly defined by the uncertainty of the measurement of the reactor thermal power. This indicates the correct modeling of both neutron fluxes and spectra, since the activation detectors with different sensitivity to thermal, epithermal, and fast neutrons were used. The deviation of the experimental and simulated values of the nuclear reaction rates, observed for the upper region of the reactor core, is about 20 %. The further improvement of the model is required while any factors, which could lead to such strong vertical asymmetry of the reactor core, are currently unknown.

5. The distribution of the flux density of thermal, epithermal, and fast neutrons along the height of the reactor core was calculated. This distribution happened to be asymmetric – its center is shifted down due to the emergency protection rods, which are present in the upper part of the reactor core, the raised control rods, and an aluminum plate at the bottom of the reactor core, which can act as a reflector.

REFERENCES

1. S. Agostinelli et al. Geant4 – a simulation toolkit. Nucl. Instrum. Meth. A 506(3) (2003) 250.
2. Neutron activation cross section measurements from threshold to 20 MeV for the validation of nuclear models and their parameters. Report number: NEA/WPEC-19. International Evaluation Co-operation, Vol. 19 (Nuclear Energy Agency, OECD Publications, 2005).

О. Г. Дьяков, І. А. Малюк, Д. П. Стратілат, М. В. Стрільчук*, В. В. Тришин

Інститут ядерних досліджень НАН України, Київ, Україна

*Відповідальний автор: myst@kinr.kiev.ua

РОЗРАХУНОК ПОТОКІВ І СПЕКТРІВ НЕЙТРОНІВ В ЕКСПЕРИМЕНТАЛЬНИХ КАНАЛАХ РЕАКТОРА ВВР-М

Розроблено програму розрахунку спектрів і щільностей потоків нейтронів в експериментальних каналах дослідницького реактора ВВР-М. Для цього було змодельовано активну зону реактора. Проведено опромінювання нейтронних активаційних детекторів. Отримані експериментальні швидкості ядерних реакцій узгоджуються з розрахованими в межах 10 %.

Ключові слова: дослідницький реактор, Geant4, спектр нейтронів, щільність потоку нейтронів, нейтронно-активаційний детектор, швидкість реакції.

Надійшла/Received 04.02.2021